



# Noise Removal Using Multi-Channel Coherence

*C.E. Lucas  
Defence R&D Canada – Atlantic*

*R. Otnes  
Norwegian Defence Research Establishment (FFI)*

**Defence R&D Canada – Atlantic**

Technical Memorandum  
DRDC Atlantic TM 2010-302  
December 2010

This page intentionally left blank.

# Noise Removal Using Multi-Channel Coherence

C.E. Lucas

Defence R&D Canada – Atlantic

R. Otnes

Norwegian Defence Research Establishment (FFI)

**Defence R&D Canada – Atlantic**

Technical Memorandum

DRDC Atlantic TM 2010-302

December 2010

Principal Author

*Original signed by C.E. Lucas*

---

C.E. Lucas

Approved by

*Original signed by Paul Hines for*

---

Dr. Dan Hutt  
Head/Underwater Sensing

Approved for release by

*Original signed by Ron Kuwahara for*

---

Dr. Calvin Hyatt  
Head/Document Review Panel

- © Her Majesty the Queen in Right of Canada as represented by the Minister of National Defence, 2010
- © Sa Majesté la Reine (en droit du Canada), telle que représentée par le ministre de la Défense nationale, 2010

## Abstract

---

In this report we show how magnetic noise occurring on an ocean floor magnetometer can be reduced using a collocated pressure sensor and a separate more distant magnetometer. To achieve this, a multi-channel coherence technique is applied to the measurement data. The removal of magnetic noise on ocean floor magnetometers has several applications, including mine warfare systems and ocean surveillance systems. Decreasing the background magnetic noise by 10-20 dB will allow the detection of a vessel magnetic field with amplitude the same order of magnitude as the background field, and with frequency content similar to that of the background field.

## Résumé

---

Dans le présent rapport, nous montrons de quelle façon le bruit magnétique enregistré à un magnétomètre posé sur le plancher océanique peut être réduit au moyen d'un capteur de pression co-implanté et d'un autre magnétomètre, situé à une certaine distance. À cette fin, on applique une technique de cohérence multicanal aux données de mesure. La suppression du bruit magnétique à des magnétomètres sur le plancher océanique a plusieurs applications, notamment en ce qui concerne les systèmes de guerre des mines et de surveillance des océans. La diminution de 10 à 20 dB du bruit magnétique de fond permettra la détection du champ magnétique d'un navire ayant une amplitude du même ordre de grandeur que le bruit de fond et un contenu en fréquence similaire à celui du champ de fond.

This page intentionally left blank.

# Executive summary

---

## Noise Removal Using Multi-Channel Coherence

C.E. Lucas, R. Otnes; DRDC Atlantic TM 2010-302; Defence R&D Canada – Atlantic; December 2010.

**Background:** The removal of background noise from bottom-mounted magnetic sensors has applications in both mine warfare and target surveillance systems. For a particular magnetic sensor, we can reduce geomagnetic and swell induced magnetic noise by using data from both a collocated pressure sensor, and a separate magnetic sensor situated approximately 100 m away. We use a multi-channel coherence technique to perform the noise removal.

**Principal results:** For frequencies below 200 mHz we show that by using the multi-channel coherence technique we can reduce background magnetic noise by up to 20 dB. Using a remote magnetometer as the first of two reference signals, we reduced the coherent background geomagnetic noise in the 5 mHz-60 mHz frequency band. As a second reference signal we used a collocated pressure sensor and reduced the swell-induced magnetic noise in the 60 mHz-200 mHz frequency band.

**Significance of results:** Decreasing the background noise on a magnetic surveillance sensor by 10-20 dB in the 5 mHz-200 mHz frequency band will allow target detection algorithms to detect surface and sub-surface targets whose magnetic signatures are typically of the same amplitude and frequency as the background noise.

**Future work:** A real-time algorithm for the implementation of the multi-channel coherence technique should be investigated. This technique should be tested under different ocean surface conditions and geomagnetic noise conditions. Determining the optimal sensor separations that maximize the noise reduction using this technique also needs to be studied.

# Sommaire

---

## Noise Removal Using Multi-Channel Coherence

C.E. Lucas, R. Otnes ; DRDC Atlantic TM 2010-302 ; R & D pour la défense Canada – Atlantique ; décembre 2010.

**Introduction :** La suppression du bruit de fond à des capteurs magnétiques posés sur le fond a des applications dans les systèmes de guerre des mines et de surveillance des cibles. Dans le cas d'un capteur magnétique particulier, nous pouvons réduire le bruit magnétique induit par la houle et géomagnétique à l'aide de données d'un capteur de pression co-implanté et d'un capteur magnétique distinct situé à environ 100 m. Nous utilisons la technique de la cohérence multicanal pour effectuer la suppression du bruit.

**Résultats :** Dans le cas des fréquences au-dessous de 200 mHz, nous montrons la technique de la cohérence multicanal nous permet de réduire le bruit magnétique de fond de jusqu'à 20 dB. En nous servant du signal d'un magnétomètre éloigné comme premier de deux signaux de référence, nous avons réduit le bruit géomagnétique de fond cohérent dans la bande de fréquences 5 mHz-60 mHz. Comme second signal de référence, nous avons utilisé un capteur de pression co-implanté et réduit le bruit magnétique induit par la houle dans la bande de fréquences 60 mHz-200 mHz.

**Portée :** La diminution du bruit de fond de 10 à 20 dB dans la bande de fréquences 5 mHz-200 mHz à un capteur de surveillance magnétique rendra possible la détection, à l'aide d'algorithmes de détection de cibles, de cibles de surface et sous-marines dont la signature magnétique est normalement de la même amplitude et de la même fréquence que le bruit de fond.

**Recherches futures :** Il faudrait explorer un algorithme en temps réel en vue de la mise en œuvre de la technique de la cohérence multicanal. Cette technique devrait être mise à l'essai dans différentes conditions de la surface de l'océan et du bruit géomagnétique. Il faut aussi étudier les moyens de déterminer la distance optimale de séparation des capteurs pour optimiser la réduction du bruit à l'aide de cette technique.



# Table of contents

---

Abstract . . . . .	i
Résumé . . . . .	i
Executive summary . . . . .	iii
Sommaire . . . . .	iv
Table of contents . . . . .	v
List of figures . . . . .	vi
1 Introduction . . . . .	1
2 Background . . . . .	2
3 Multi-Channel Coherence . . . . .	3
3.1 Mathematical Development . . . . .	4
4 Analysis of Experimental Data . . . . .	6
5 Conclusions . . . . .	13
References . . . . .	15

# List of figures

---

Figure 1:	Signal flow diagram for the mathematical model relating the test signal $Y$ to two input signals $X_1$ and $X_2$ . . . . .	3
Figure 2:	Norwegian Herdla range sensor positions. . . . .	5
Figure 3:	Coherence between $Bz_E(t)$ and the pressure signal $P_E(t)$ , East sensor group. . . . .	7
Figure 4:	Coherence between vertical magnetic fields $Bz_E(t)$ and $Bz_M(t)$ . . . . .	8
Figure 5:	Multi-channel coherence between $Bz_E(t)$ and both $Bz_M(t)$ , $P_E(t)$ . . . . .	9
Figure 6:	Original time series $y(t) = Bz_E(t)$ and the calculated residual signal $e(t)$ . . . . .	10
Figure 7:	Power spectral densities $S_{yy}(f)$ and $S_{ee}(f)$ of the signals $y(t) = Bz_E(t)$ and $e(t)$ . . . . .	10
Figure 8:	The degree of cancellation (dB) between $y(t) = Bz_E(t)$ and both signals $x_1(t) = Bz_M(t)$ , $x_2(t) = P_E(t)$ . . . . .	11

# 1 Introduction

---

Ocean bottom-mounted magnetometers are used extensively in oceanic surveillance systems [1]. These systems are mostly deployed in water depths no more than a few hundred meters. Surveillance systems typically consist of an array of sensors, or multi-sensor platforms, spaced according to the particular application, such as port access or deep water choke point surveillance. The underwater sensors or platforms are usually cabled to each other and/or cabled to shore. In such connected arrays the data from all sensors is available at each sensor or onshore immediately. Signal processing methods can take advantage of having all the sensor data from all channels available, and can be used to reduce unwanted noise from particular channels of interest.

Most surface and sub-surface ocean vessels have both permanent and induced magnetization within their structures. This magnetization produces an associated magnetic field, often referred to as a signature, that can be sensed by modern magnetometers at hundreds of meters range. When a vessel transits near a magnetometer, the magnetometer measures the vessel's quasi-static magnetic field, which varies only with time as the vessel moves relative to the fixed sensor.

Underwater surveillance systems that employ magnetometers use signal processing algorithms to detect magnetic signatures from nearby vessels. Reducing the effective background noise on the magnetometer measurements will allow the algorithms to detect smaller target signatures that otherwise would have been hidden in the background noise.

The magnetic signature produced from a transiting vessel measured by a bottom-mounted magnetometer lies predominantly in the frequency band from approximately 5 mHz to 200 mHz. Within this frequency band there are two dominant sources of background magnetic noise, geomagnetic and ocean swell induced [2, 3]. Geomagnetic noise is due to electrical currents deep within the Earth, as well as interactions between the solar wind and the geomagnetic field. It is well known that geomagnetic noise has high spatial coherence over many hundreds of meters and even kilometers [4]. We can take advantage of the coherence if we have multiple magnetic sensors with sensor separations on the order of 100 m or more, with one sensor in the same vicinity of the vessel.

Ocean swell induced magnetic noise is due to eddy currents arising from the movement of sea water, and the associated charged particles, in the Earth's magnetic field during swell activity. These electrical currents have a corresponding magnetic field associated with them which contributes to the noise measured on ocean-bottom magnetometers. It has been established that there is a physical relationship between the swell induced magnetic noise and the local hydrostatic pressure at the sensor location [5] [6].

In this report we describe the use of a multi-channel coherence technique to reduce background noise on the vertical magnetic field measured from a bottom-mounted magnetome-

ter (our test signal). We use measurements of the local swell-induced pressure signal, and the magnetic field from a separate magnetometer approximately 100 m away, as additional input data for the multi-channel coherence technique. By using these signals we were able to reduce the magnetic noise on our test signal by up to 20 dB in the 5 mHz-200 mHz frequency band.

## 2 Background

---

Consider a vessel transiting within measurement range of a bottom-mounted magnetometer in water at depth on the order of 100 m. We consider this sensor to be our test sensor, and the measured vertical magnetic field our test signal. The measured magnetic field is the sum of the target magnetic signature, the geomagnetic background, and the swell-induced magnetic noise.

To reduce the background noise on the test signal, we use the local hydrostatic pressure signal, and the vertical magnetic field measured at a distant magnetometer approximately 100 m away. Using the multi-channel coherence technique, we can remove from our test signal all signal components that are coherent with both the collocated pressure signal and the distant magnetometer signal. We will refer to the local pressure and distant magnetometer signals as our reference signals. Ideally the reference signals will only have coherence with the unwanted background noise on the test signal.

To apply this technique to the detection of a vessel's magnetic field, we take advantage of the field's rapid decay with range  $R$ . The magnetic field of a vessel can be accurately represented as that produced by one or more magnetic dipoles. The resulting magnetic field amplitude decreases with range at least as fast as  $1/R^3$ . For a vessel transiting near our test sensor, the associated vessel magnetic field 100 m or more away will be significantly reduced, possibly completely hidden in the noise or below the sensor resolution, because of the decay with range. If this is the case, the remote sensor signal will consist mostly of geomagnetic and swell-induced magnetic noise. If we have access to the remote magnetic signal, we can use the multi-channel coherence technique to remove from our test signal those components that are coherent with the remote signal. Since geomagnetic noise has high spatial coherence over large ranges, we will be able to reduce the geomagnetic noise significantly from our test signal.

Transiting surface vessels produce a small pressure signal, which can be detected in shallow water in calm low-swell conditions by a pressure sensor. This pressure signal decreases rapidly with range, and is often undetectable even in low swell conditions. The local swell pressure usually dominates the pressure sensor signal. Additionally, the pressure signature of a vessel typically has low coherence with its magnetic signature. If we assume our pressure sensor is at a depth where the pressure signature of the vessel is small or incoherent with its magnetic signature, we can then safely use the measured pressure to remove

the coherent swell-induced magnetic signal from our magnetic test signal. As described in [5] [6], the swell-induced magnetic noise is coherent with the local pressure signal produced by the swell. We use measurements of the swell pressure, and take advantage of its coherence with the swell-induced magnetic noise, as in [2], to remove this noise from our test signal. The method described here however differs from [2] in that we use both the local pressure signal *and* a remote magnetometer, and use a multi-channel coherence function to reduce the noise on the test signal. Using the multi-channel coherence technique we simultaneously remove from our test signal all signals that are coherent with the local pressure signal, and the remote (100 m) magnetic signal. This reduces the noise on the test signal and makes the vessel magnetic signature easier to detect using a detection algorithm.

### 3 Multi-Channel Coherence

A multi-channel coherence function can be used to remove signal components from a test signal that are coherent with multiple other signals [7]. Figure 1 shows the signal flow diagram for the mathematical model relating a test channel  $Y$  and two separate signals  $X_1$  and  $X_2$  that are coherent with  $Y$ . In the signal flow diagram capital letters denote the frequency domain representation of the signals. The functions  $H_1$  and  $H_2$  represent the linear system transfer functions that relate the two input signals  $X_1, X_2$  to the output signal  $Y$ . As seen in Figure 1 the signal  $V$  is the sum of the outputs of the two transfer functions, and signal  $Y$  is the sum of signals  $V$  and  $E$ . The residual signal  $E$  is that part of signal  $Y$  that is not coherent with  $X_1, X_2$ , and signal  $V$  is that part of signal  $Y$  that is coherent with  $X_1, X_2$ .

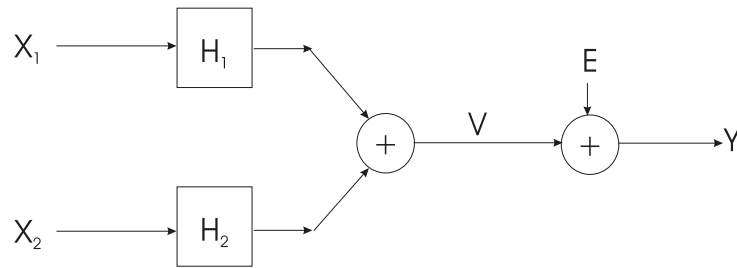


**Figure 1:** Signal flow diagram for the mathematical model relating the test signal  $Y$  to two input signals  $X_1$  and  $X_2$ .

The concept of application for this method is that signal  $Y$  is the measured vertical magnetic field of a target vessel plus magnetic noise associated with geomagnetism and ocean swell. We will associate signal  $X_1$  with the local pressure signal, and signal  $X_2$  with the vertical magnetic field from a reference magnetometer. We assume the target magnetic signature at the reference sensor will be very small, or not coherent, with the local vessel signature contained in  $Y$ . The residual signal  $E$  will contain the vessel signature contained in  $Y$  with

all coherent signals from  $X_1$  and  $X_2$  removed. A target detection algorithm for magnetic signatures would be applied to the time-domain representation of signal  $E$ .

### 3.1 Mathematical Development

Using cross-spectral relationships between the signal  $Y$  and the two input signals  $X_1, X_2$  in Figure 1, we can obtain estimates of the transfer functions  $H_1, H_2$ . The cross-spectra between signals  $E$  and  $X_1, E$  and  $X_2$ , and  $E$  and  $V$  are zero by definition of the model. We denote the cross-spectra as defined in [7] between any two signals  $X$  and  $Y$  by  $S_{xy}$ . Taking the cross-spectra between  $Y$  and the two input signals  $X_1, X_2$  we obtain:

$$\begin{aligned} S_{x_1y}(f) &= S_{x_1x_1}(f)H_1(f) + S_{x_1x_2}(f)H_2(f) \\ S_{x_2y}(f) &= S_{x_2x_1}(f)H_1(f) + S_{x_2x_2}(f)H_2(f). \end{aligned} \quad (1)$$

Using the cross- and auto-spectra obtained from the measured data, equations 1 are solved for the unknown transfer functions  $H_1, H_2$ . Using the estimates for  $H_1, H_2$ , we calculate the power spectral density for signal  $V$  from

$$\begin{aligned} S_{vv}(f) &= S_{x_1x_1}(f)|H_1(f)|^2 + S_{x_2x_2}(f)|H_2(f)|^2 + 2\Re\{S_{x_2x_1}(f)H_1(f)H_2^*(f)\} \\ &= S_{x_1y}(f)H_1^*(f) + S_{x_2y}(f)H_2^*(f). \end{aligned} \quad (2)$$

Here  $*$  represents the complex conjugate. Since  $S_{yv}(f) = S_{vv}(f)$ , and  $S_{vv}(f) = (S_{vv}(f))^*$ , we can define the multi-channel coherence function between  $Y$  and all inputs  $X_i$  as

$$\gamma_{y:x_i}^2(f) = \frac{|S_{yv}(f)|^2}{S_{yy}(f)S_{vv}(f)} = \frac{(S_{vv}(f))^*S_{vv}(f)}{S_{yy}(f)S_{vv}(f)} = \frac{S_{vv}(f)}{S_{yy}(f)}. \quad (3)$$

With this definition for the multi-channel coherence, we can calculate the power spectral density of the residual signal  $E$  from

$$S_{ee}(f) = S_{yy}(f) - S_{vv}(f) = (1 - \gamma_{y:x_i}^2(f))S_{yy}(f). \quad (4)$$

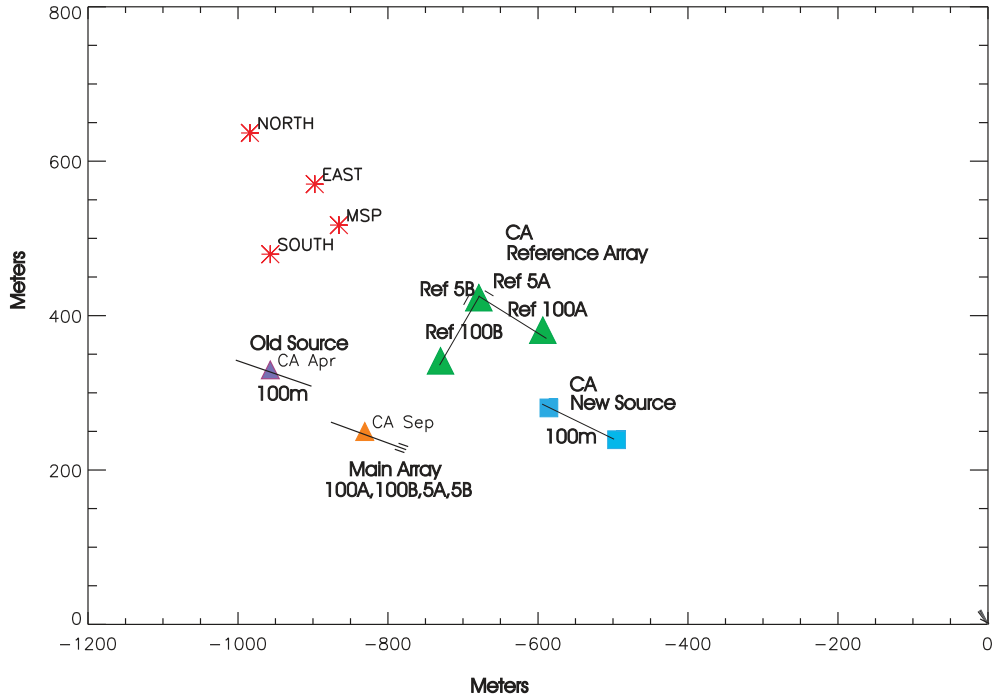


**Figure 2:** Norwegian Herdla range sensor positions. Stars denote the permanently installed Norwegian sensor groups North, South, East, and MSP. Other symbols denote sources and sensors deployed by DRDC Atlantic.

The time domain residual signal  $e(t)$  may be calculated from the frequency domain functions using the Inverse Fourier Transform ( $F^{-1}$ ).

$$e(t) = F^{-1}\{Y(f) - X_1(f)H_1(f) - X_2(f)H_2(f)\} \quad (5)$$

We refer to the signal  $e(t)$  as the residual time series that results from “cancelling” the output signal  $y(t)$  against the input signals  $x_1(t)$ ,  $x_2(t)$ .

The multi-channel coherence technique may be generalized to  $N$  inputs  $x_i(t)$ ,  $i = 1..N$ , allowing further cancellation using other signals that have coherence with the test signal  $y(t)$ . Ideally these other signals will not be coherent with any target signature contained in  $y(t)$ . In a multi-sensor surveillance application this generalization to more inputs could have a significant benefit by reducing unwanted noise on multiple sensors simultaneously.

## 4 Analysis of Experimental Data

---

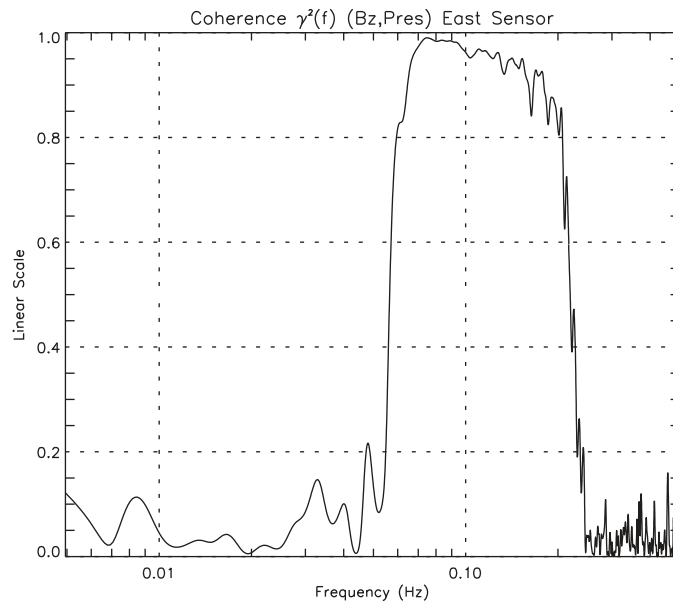
Experimental data was collected at the Next Generation Autonomous Systems (NGAS) Joint Research Project trial held in Norway in September 2004. The trial took place at the Norwegian Herdla sensor range in Hjeltefjorden, northwest of Bergen.

Figure 2 shows the physical layout of the Herdla range sensor groups dubbed North, South, East, and MSP that were used for the collection of the data. These sensor groups are multi-influence platforms that include tri-axial magnetometers and hydrostatic pressure sensors. The sensor groups are spaced over 100 m apart from each other, and their depths range from approximately 20-85 m: North (49.9 m), East (26.7 m), South (84.2 m) and MSP (21.0 m). The data used in this analysis was collected on September 24th, 2004 and is 118 minutes in length. During these measurements, there was a gale with wind speeds of 15-20 m/s.

For the data collected in this experiment we used a sample rate of 1.0 Hz. The total number of time samples analyzed per sensor was  $NT = 7 * 1024 = 7168$ . A total of 13 1024-point data segments with 50% overlap were used to estimate the required spectra using the Fast Fourier Transform (FFT) and Welch's Method. Each 1024-point data segment was windowed using a Hanning window, then zero-padded to a length of  $NT$  points before taking the FFT. The resulting spectra were then averaged over the 13 segments to obtain the required auto- and cross-spectra. Thus all spectral estimates in equations 1 through 5 including the transfer functions  $H_1(f)$  and  $H_2(f)$  are  $NT$  frequency points in length. The spectra  $X_1(f)$ ,  $X_2(f)$  and  $Y(f)$  are obtained by taking the  $NT$ -point FFT of each of the corresponding time series.

In our analysis we use as our test channel the vertical magnetic field  $Bz_E(t)$  measured from the Herdla East sensor group. From this channel we remove signal content that is coherent with those signals measured simultaneously from the East sensor group pressure sensor  $P_E(t)$  and also from the MSP vertical magnetic sensor  $Bz_M(t)$ . We relate our measured data with the signal flow diagram of Figure 1 by assigning  $y(t) = Bz_E(t)$ ,  $x_1(t) = P_E(t)$ , and  $x_2(t) = Bz_M(t)$ .





**Figure 3:** Coherence between  $Bz_E(t)$  and the pressure signal  $P_E(t)$ , East sensor group.

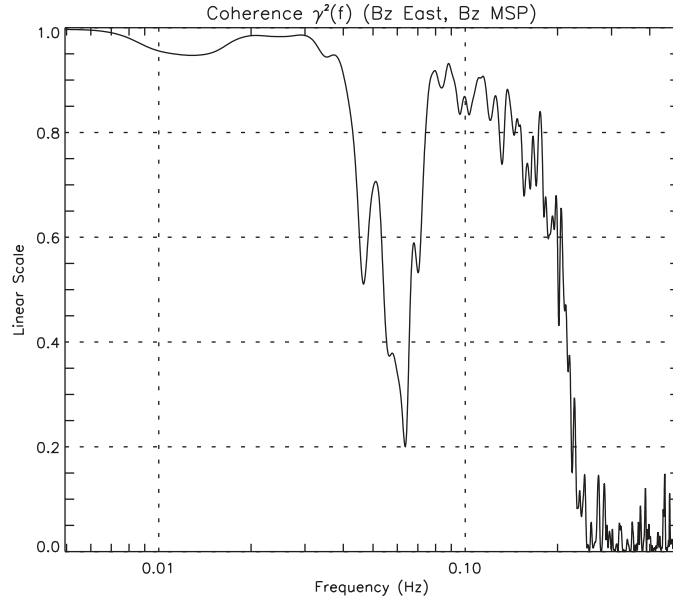


**Figure 4:** Coherence between vertical magnetic fields  $B_{zE}(t)$  and  $B_{zM}(t)$ .

The measured data at the East sensor group shows a physical relationship between the local swell induced magnetic noise and the pressure signal. This relationship is apparent in Figure 3 where we have a high degree of coherence between the vertical magnetic field  $B_{zE}(t)$  and the Pressure signal  $P_E(t)$  at the East sensor group, particularly in the 60 mHz to 200 mHz frequency band. Here we have used the coherence function  $\gamma_{y:x}^2(f)$  between two signals  $x(t), y(t)$ , defined in terms of their auto- and cross-spectra as

$$\gamma_{y:x}^2(f) = \frac{|S_{xy}(f)|^2}{S_{xx}(f)S_{yy}(f)}. \quad (6)$$

In Figure 4 we show the coherence between the vertical magnetic fields  $B_{zE}(t)$  and  $B_{zM}(t)$ . The horizontal distance between these sensor groups is approximately 100 m. The high coherence below 60 mHz is due to the high spatial coherence of the geomagnetic noise in this frequency band over the sensor group separation. Geomagnetic noise below 60 mHz can show high coherence over several kilometers.

In Figure 5 we show the multi-channel coherence between  $B_{zE}(t)$  and both  $B_{zM}(t)$  and  $P_E(t)$ , defined by equation 3. The multi-channel coherence is high in both the geomagnetic and the pressure swell noise frequency bands, and extends in frequency up to 200 mHz. Using equation 5, we can solve for the residual time series  $e(t)$ . Here  $e(t)$  is the East sensor group vertical magnetic field  $B_{zE}(t)$  with the coherent noise from  $B_{zM}(t)$  and  $P_E(t)$

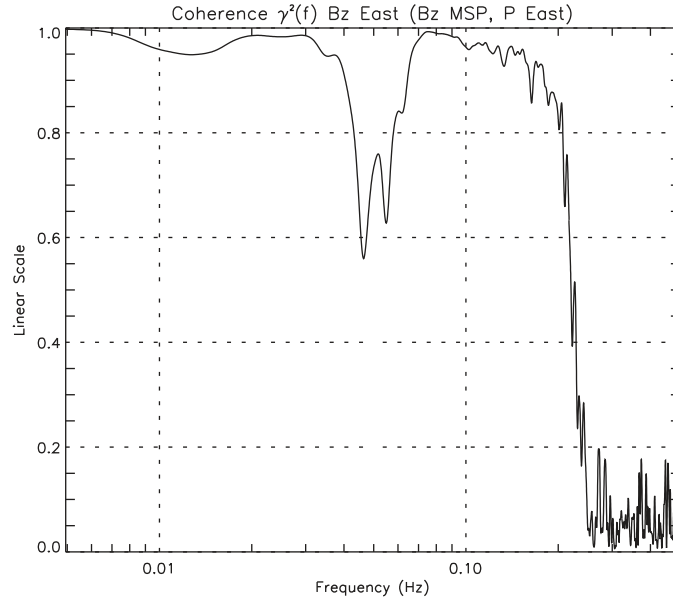


**Figure 5:** Multi-channel coherence between  $B_{zE}(t)$  and both  $B_{zM}(t)$ ,  $P_E(t)$ .

removed. In Figure 6 we compare the residual signal  $e(t)$  with the original vertical magnetic field test signal  $y(t)$ . Figure 6 clearly shows that a target signature of only a few nano-Tesla can be easily detected in the residual signal  $e(t)$ . There were no target transits in this data set.

Figure 7 shows the corresponding power spectral densities  $S_{yy}(f)$ ,  $S_{ee}(f)$  of the original test channel  $y(t) = B_{zE}(t)$  and the residual signal  $e(t)$  after performing the cancellation with the signals  $x_1(t) = B_{zM}(t)$  and  $x_2(t) = P_E(t)$ . In Figure 8 we show the degree of cancellation between  $y(t) = B_{zE}(t)$  and both  $x_1(t) = B_{zM}(t)$  and  $x_2(t) = P_E(t)$ . The degree of cancellation is defined to be the difference in the decibel values of  $S_{yy}(f)$  and  $S_{ee}(f)$  of Figure 7. It is the multiplying factor increase in SNR, expressed in decibels, resulting from the noise removal. Up to 20 dB of noise has been removed from the measured vertical magnetic field in the 5 mHz to 200 mHz frequency band. This frequency band corresponds to that associated with the magnetic signature of a transiting vessel measured from a bottom-mounted magnetometer. A target detection algorithm applied to the residual signal  $e(t)$  will have greater detection capability due to the factor of 10 (20 dB) increase in SNR. This applies to the detection of both nearby vessels with small magnetic source strengths, and vessels with larger magnetic source strengths that are at a greater distance away.

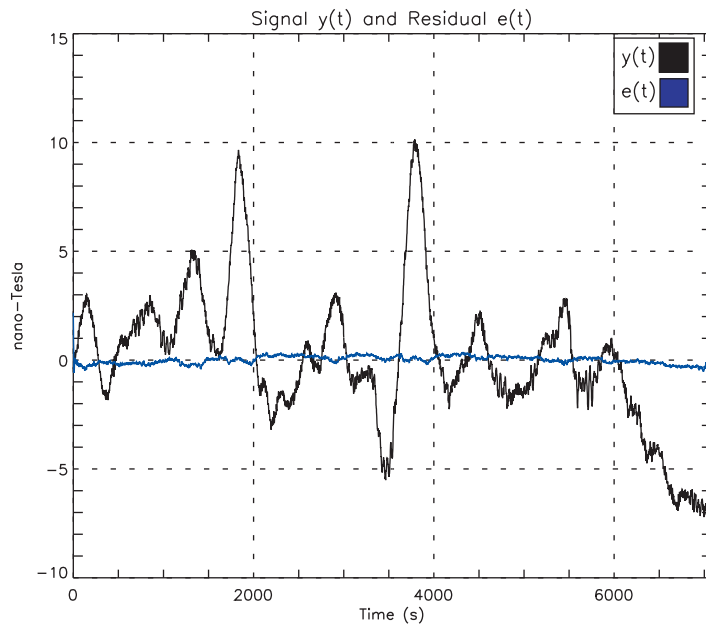


**Figure 6:** Original time series  $y(t) = B_{zE}(t)$  and the calculated residual signal  $e(t)$  with coherent signals from  $B_{zM}(t)$ ,  $P_E(t)$  removed. A target magnetic signature of only a few nano-Tesla could now be easily detected on  $e(t)$ .

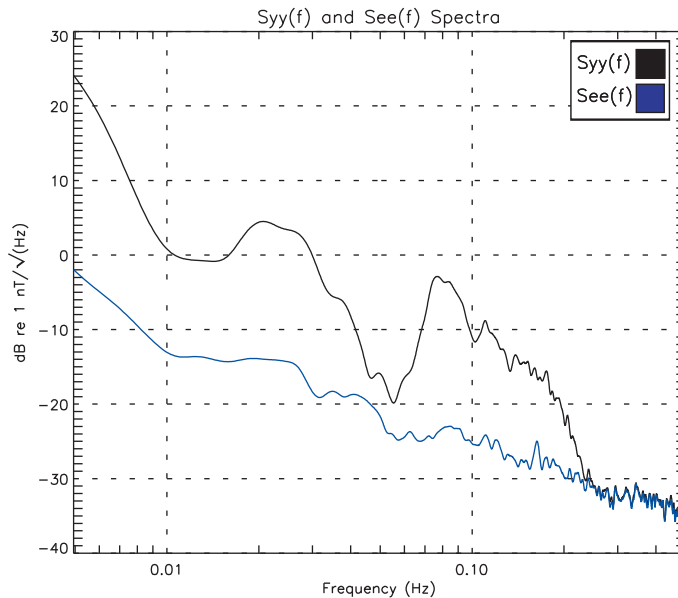


**Figure 7:** Power spectral densities  $S_{yy}(f)$  and  $S_{ee}(f)$  of the signals  $y(t) = B_{zE}(t)$  and  $e(t)$ .

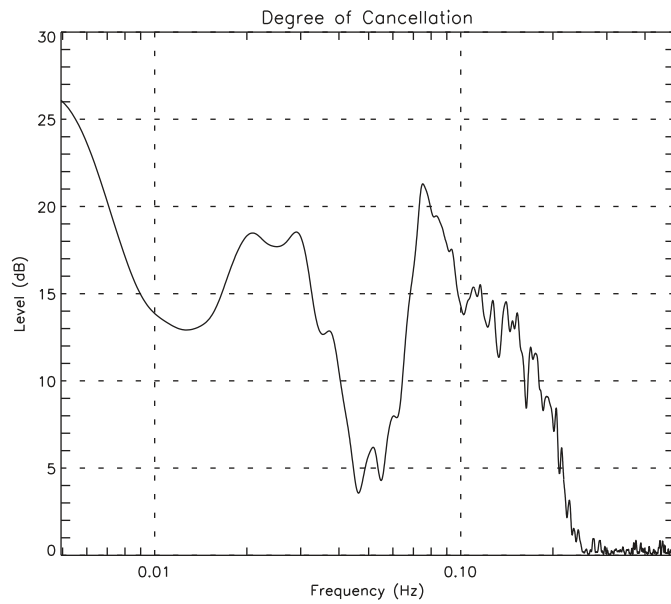


**Figure 8:** The degree of cancellation (dB) between  $y(t) = Bz_E(t)$  and both signals  $x_1(t) = Bz_M(t)$ ,  $x_2(t) = P_E(t)$ . This measure is the multiplying factor increase in SNR, expressed in decibels, resulting from the noise removal.

To optimize the performance of the multi-channel coherence technique in reducing noise on the test signal, without also reducing the target signature within the test signal, the reference signals must be chosen carefully. If possible the reference signals should be chosen such that they are coherent with the background noise on the test signal, and not coherent with the vessel signature of interest. This is likely to be true in practical scenarios based on the concept of usage described here because:

1. The detection range of pressure signatures is known to be much smaller than that of magnetic signatures. For a surveillance array deployed at depths greater than 20 m, the target pressure signal from a collocated pressure sensor will be dominated by the local pressure swell. The pressure signal will have no coherence with the target magnetic signal on the test sensor.
2. For the magnetic signal, our reference signal would contain very little of the target magnetic signature because of the rapid fall-off rate with range of the magnetic field. Essentially the target signature is not present at both sensors simultaneously. The remote reference signal should then only consist of background geomagnetic and ocean-swell induced magnetic noise, and be incoherent with the target magnetic signature.

## 5 Conclusions

---

We have shown that the multi-channel coherence technique can be effective in reducing unwanted noise on a test signal by removing those signal components that are coherent with other available signals. For a test signal we used the vertical magnetic field measured from a bottom-mounted magnetometer. Using a collocated pressure sensor, and a vertical magnetic field sensor 100 m away as reference signals, we were able to reduce the background magnetic noise on our test signal by approximately 18 dB in the frequency band from 5 mHz to 200 mHz. The pressure reference signal was used to reduce the coherent swell induced magnetic background noise in the 60 mHz to 200 mHz band, and the magnetic reference signal was used to reduce the geomagnetic background noise in the 5 mHz to 60 mHz band.

The magnetic signature of a transiting surface vessel as measured by a bottom-mounted magnetometer is typically in the 5 mHz to 200 mHz frequency band. By decreasing the noise on our test channel by 18 dB in this band, target detection algorithms may be applied with lower detection thresholds, and target signals almost an order of magnitude smaller than previously will be able to be detected. This will increase the detection capability of the surveillance array using this technique, and decrease false alarms produced by background noise fluctuations.

For surveillance applications where we have an array of sensors or multi-sensor platforms cabled together and distributed on the ocean bottom, the multi-channel coherence technique has great potential for reducing background noise on the returned sensor data. For cabled arrays, all data from all sensor may be available simultaneously. Array sensors placed in areas where target vessels are unlikely to transit near could be used as reference sensors for the other array sensors more likely to have a target pass nearby. For surveillance arrays cabled to shore, a completely separate reference array could be deployed in an area where targets are unlikely to pass. This reference data could be then used to reduce noise on sensor data collected from a main array deployed in the target transit area.

If a surveillance array has distributed multi-sensor platforms that are not cabled together, the multi-channel coherence technique can still be used to reduce noise. We have shown that by using a collocated pressure sensor we were able to reduce the background noise on a magnetic signal. Other collocated sensors, such as three-component electric field sensors, could also be used if they show any coherence with the background noise on the test signal.

It should be made clear that the multi-channel coherence technique is not just about reducing background noise on a magnetic signal. We could just as easily be measuring electric fields or acoustic signals, and trying to reduce the background noise on these signals by using the appropriate reference sensors.

Future work needs to be performed to determine the optimal sensor distribution for a surveillance array if the multi-channel noise removal technique were used. This would depend on the surveillance application, and in particular depend on such things as; the deployment depth, the target fields (magnetic, electric, acoustic etc.) to be sensed, the expected source strengths of the targets, the different expected weather conditions, the tidal conditions and the geomagnetic noise conditions.

From a computational perspective, future work could also be performed in analyzing the resulting linear system transfer functions that the model produces. Preliminary study of these functions has shown that once they have been calculated, they can be used without having to update them at every computation time window. These functions, which in a way characterize the local environment, have some temporal stability. If this is indeed the case, then this will greatly reduce the amount of computation time required to implement the multi-channel coherence technique in a real-time application. A study of the temporal stability of the transfer functions should be performed.



## References

---

- [1] Holmes, J. J. (2006), *Exploitation of a Ship's Magnetic Field Signatures*, 1 ed, San Rafael, CA: Morgan & Claypool Publishers,.
- [2] Otnes, R. (2005), *Suppression of Swell Noise in Underwater Magnetic Measurements Using Collocated Pressure Sensors*, In *Proc. UDT Europe 2005*, Amsterdam, Netherlands.
- [3] Otnes, R., Lucas, C., and Holtham, P. (2006), *Noise Suppression Methods in Underwater Magnetic Measurements*, In *Proc. Marelec 2006*, Amsterdam, Netherlands.
- [4] Nelson, B. J. (2007), *Geological and Geomagnetic Noise Reduction Along the Atlantic Continental Margin*. DRDC Atlantic Technical Memorandum 2007-002.
- [5] Weaver, J. (Apr. 1965), *Magnetic variations associated with ocean waves and swell*, *Geophys. Res.*, vol. 70, pp. 1921–1929.
- [6] Podney, W. (July 1975), *Electromagnetic fields generated by ocean waves*, *Geophys. Res.*, vol. 80, pp. 2977–2990.
- [7] Bendat, J. S. and Piersol, A. G. (1980), *Engineering Applications of Correlation and Spectral Analysis*, 1 ed, New York, NY: John Wiley and Sons,.

This page intentionally left blank.

# Distribution list

---

DRDC Atlantic TM 2010-302

## Internal distribution

- 1 C. Lucas, DRDC Atlantic
- 1 G. Heard, DRDC Atlantic
- 1 N. Pelavas, DRDC Atlantic
- 1 Z. Daya, DRDC Atlantic
- 1 T. Richards, DRDC Atlantic
- 3 Library, DRDC Atlantic

**Total internal copies: 8**

## External distribution

- 1 DRDKIM
- 1 Library and Archives Canada (Attn: Military Archivist, Government Records Branch)
- 1 Roald Otnes, Norwegian Defence Research Establishment, Maritime Systems Division, PO Box 115, NO-3191 Horten, Norway

**Total external copies: 3**

**Total copies: 11**

This page intentionally left blank.

<b>DOCUMENT CONTROL DATA</b>		
<small>(Security classification of title, body of abstract and indexing annotation must be entered when document is classified)</small>		
<p>1. ORIGINATOR (The name and address of the organization preparing the document. Organizations for whom the document was prepared, e.g. Centre sponsoring a contractor's report, or tasking agency, are entered in section 8.)</p> <p><b>Defence R&amp;D Canada – Atlantic PO Box 1012, Dartmouth, NS, Canada B2Y 3Z7</b></p>	<p>2. SECURITY CLASSIFICATION (Overall security classification of the document including special warning terms if applicable.)</p> <p><b>UNCLASSIFIED</b></p>	
<p>3. TITLE (The complete document title as indicated on the title page. Its classification should be indicated by the appropriate abbreviation (S, C or U) in parentheses after the title.)</p> <p><b>Noise Removal Using Multi-Channel Coherence</b></p>		
<p>4. AUTHORS (Last name, followed by initials – ranks, titles, etc. not to be used.)</p> <p><b>Lucas, C. E.; Otnes, R.</b></p>		
<p>5. DATE OF PUBLICATION (Month and year of publication of document.)</p> <p><b>December 2010</b></p>	<p>6a. NO. OF PAGES (Total containing information. Include Annexes, Appendices, etc.)</p> <p><b>28</b></p>	<p>6b. NO. OF REFS (Total cited in document.)</p> <p><b>7</b></p>
<p>7. DESCRIPTIVE NOTES (The category of the document, e.g. technical report, technical note or memorandum. If appropriate, enter the type of report, e.g. interim, progress, summary, annual or final. Give the inclusive dates when a specific reporting period is covered.)</p> <p><b>Technical Memorandum</b></p>		
<p>8. SPONSORING ACTIVITY (The name of the department project office or laboratory sponsoring the research and development – include address.)</p> <p><b>Defence R&amp;D Canada – Atlantic PO Box 1012, Dartmouth, NS, Canada B2Y 3Z7</b></p>		
<p>9a. PROJECT OR GRANT NO. (If appropriate, the applicable research and development project or grant number under which the document was written. Please specify whether project or grant.)</p> <p><b>Next Generation Autonomous Systems (NGAS) NATO Joint Research Project</b></p>	<p>9b. CONTRACT NO. (If appropriate, the applicable number under which the document was written.)</p>	
<p>10a. ORIGINATOR'S DOCUMENT NUMBER (The official document number by which the document is identified by the originating activity. This number must be unique to this document.)</p> <p><b>DRDC Atlantic TM 2010-302</b></p>	<p>10b. OTHER DOCUMENT NO(s). (Any other numbers which may be assigned this document either by the originator or by the sponsor.)</p>	
<p>11. DOCUMENT AVAILABILITY (Any limitations on further dissemination of the document, other than those imposed by security classification.)</p> <p><input checked="" type="checkbox"/> Unlimited distribution</p> <p><input type="checkbox"/> Defence departments and defence contractors; further distribution only as approved</p> <p><input type="checkbox"/> Defence departments and Canadian defence contractors; further distribution only as approved</p> <p><input type="checkbox"/> Government departments and agencies; further distribution only as approved</p> <p><input type="checkbox"/> Defence departments; further distribution only as approved</p> <p><input type="checkbox"/> Other (please specify):</p>		
<p>12. DOCUMENT ANNOUNCEMENT (Any limitation to the bibliographic announcement of this document. This will normally correspond to the Document Availability (11). However, where further distribution (beyond the audience specified in (11)) is possible, a wider announcement audience may be selected.)</p>		

13. ABSTRACT (A brief and factual summary of the document. It may also appear elsewhere in the body of the document itself. It is highly desirable that the abstract of classified documents be unclassified. Each paragraph of the abstract shall begin with an indication of the security classification of the information in the paragraph (unless the document itself is unclassified) represented as (S), (C), or (U). It is not necessary to include here abstracts in both official languages unless the text is bilingual.)

In this report we show how magnetic noise occurring on an ocean floor magnetometer can be reduced using a collocated pressure sensor and a separate more distant magnetometer. To achieve this, a multi-channel coherence technique is applied to the measurement data. The removal of magnetic noise on ocean floor magnetometers has several applications, including mine warfare systems and ocean surveillance systems. Decreasing the background magnetic noise by 10-20 dB will allow the detection of a vessel magnetic field with amplitude the same order of magnitude as the background field, and with frequency content similar to that of the background field.

14. KEYWORDS, DESCRIPTORS or IDENTIFIERS (Technically meaningful terms or short phrases that characterize a document and could be helpful in cataloguing the document. They should be selected so that no security classification is required. Identifiers, such as equipment model designation, trade name, military project code name, geographic location may also be included. If possible keywords should be selected from a published thesaurus. e.g. Thesaurus of Engineering and Scientific Terms (TEST) and that thesaurus identified. If it is not possible to select indexing terms which are Unclassified, the classification of each should be indicated as with the title.)

Coherence  
Noise Removal  
Cancellation  
Magnetometer  
Pressure

This page intentionally left blank.

## **Defence R&D Canada**

Canada's leader in defence  
and National Security  
Science and Technology

## **R & D pour la défense Canada**

Chef de file au Canada en matière  
de science et de technologie pour  
la défense et la sécurité nationale



[www.drdc-rddc.gc.ca](http://www.drdc-rddc.gc.ca)